

RESEARCH

Open Access



# The effects of restorative material and connector cross-section area on the stress distribution of fixed partial denture: a finite element analysis

Jingyi Chen<sup>1†</sup>, Tong Zhu<sup>1†</sup>, Ruyi Li<sup>2</sup>, Zhou Zhu<sup>1</sup>, Xibo Pei<sup>1</sup>, Yichen Xu<sup>1\*</sup> and Qianbing Wan<sup>1\*</sup>

## Abstract

**Background** This study aimed to evaluate the effects of restorative materials and connector cross-section areas (CSAs) on the stress distribution of monolithic fixed partial dentures (FPDs).

**Methods** FPDs, abutment teeth, periodontal ligament (PDL), and alveolar bone were modeled by computer-aided design. Four materials with varied elastic modulus (3 mol% yttria-stabilized tetragonal zirconia polycrystals [Zr], lithium disilicate [LD], polymer-infiltrated ceramic network [PICN], and resin composite [RC]) and five CSA of connectors (4, 6, 8, 10, and 12 mm<sup>2</sup>) were set as FPD variables for finite element analysis (FEA). The stress distribution on FPDs, abutment teeth, PDL, and alveolar bone was analyzed under two different loading modes (three-point loading and pontic loading). The results of FEA were further verified by photoelastic test.

**Results** Both FPD material and CSA influenced the stress distribution of the FPD-tooth-bone complex. At a constant CSA of 8 mm<sup>2</sup>, Zr, with the highest elastic modulus, exhibited the lowest stress on abutment teeth (2.4177 MPa). As the materials' elastic modulus decreased, the stress increased by 2.37%, 7.67%, and 13.16% for LD, PICN, and RC, respectively. Increasing the CSA from 4 mm<sup>2</sup> to 12 mm<sup>2</sup> reduced stress on abutments by 1.65% and 1.54% in the Zr and PICN groups, respectively. However, in the RC group, the stress increased significantly by 115.63%.

**Conclusion** Materials with a higher elastic modulus tend to confine stress within the FPDs, reducing the downward transmission of stress. As the CSA increases, stress might be more evenly distributed from FPD to the periodontium, potentially reducing stress concentration.

**Keywords** Stress distribution, Finite element analysis, Fixed partial denture, Elastic modulus, Connector

<sup>†</sup>Jingyi Chen and Tong Zhu contributed equally to this work.

\*Correspondence:

Yichen Xu

yichen.xu@scu.edu.cn

Qianbing Wan

champion@scu.edu.cn

<sup>1</sup>State Key Laboratory of Oral Diseases & National Center for Stomatology & National Clinical Research Center for Oral Diseases & Frontier Innovation

Center for Dental Medicine Plus, Department of Oral Prosthodontics I, West China Hospital of Stomatology, Sichuan University, Chengdu 610041, China

<sup>2</sup>State Key Laboratory of Oral Diseases & National Center for Stomatology & National Clinical Research Center for Oral Diseases & Frontier Innovation Center for Dental Medicine Plus, Department of Dental Technology, West China Hospital of Stomatology, Sichuan University, Chengdu 610041, China



© The Author(s) 2025. **Open Access** This article is licensed under a Creative Commons Attribution-NonCommercial-NoDerivatives 4.0 International License, which permits any non-commercial use, sharing, distribution and reproduction in any medium or format, as long as you give appropriate credit to the original author(s) and the source, provide a link to the Creative Commons licence, and indicate if you modified the licensed material. You do not have permission under this licence to share adapted material derived from this article or parts of it. The images or other third party material in this article are included in the article's Creative Commons licence, unless indicated otherwise in a credit line to the material. If material is not included in the article's Creative Commons licence and your intended use is not permitted by statutory regulation or exceeds the permitted use, you will need to obtain permission directly from the copyright holder. To view a copy of this licence, visit <http://creativecommons.org/licenses/by-nc-nd/4.0/>.

## Background

Fixed partial denture (FPD) is a type of the fixed prosthodontic restoration used to rehabilitate small-scale dentition defects by permanently anchoring to adjacent natural teeth. Three-unit fixed bridges represent the most common form of FPDs, providing an effective treatment alternative for patients who are either unwilling to undergo implant surgery, have medical contraindications, or face financial constraints [1]. The clinical success of FPDs depends, among other factors, on their ability to effectively withstand the complex forces present in the oral cavity [2], including compressive, tensile, and shear loads [3]. Owing to various resistance ability of constituents in FPD-teeth-bone complex, the stress distribution is often inhomogeneous. Imbalanced stress distribution may lead to adhesive failure, dental caries, pulp irritation, excessive wear of the opposing tooth, and even result in the fracture of the restoration, marginal bone loss of abutment teeth, and prolonged discomfort for the patient [4, 5]. Thus, it is necessary to develop a rational stress distribution based on the mechanical properties of each component.

To achieve this objective, careful consideration must be given to the structural design and material selection of FPDs. On one hand, the structural design of FPDs should optimize load distribution by adjusting the resistance form. Among the various factors, the cross-section area (CSA) of connectors might be critical, as connectors are frequently associated with stress concentration and FPD fracture [6, 7]. Moreover, previous studies have demonstrated that reducing the CSA of connectors could increase the stress on the periodontal tissues of abutment teeth [7, 8]. Studart et al. indicated that 3 mol% yttria-stabilized tetragonal zirconia polycrystals (3Y-TZP)-based 3-unit bridges should have a CSA of connectors no less than 4.9 mm<sup>2</sup> [9]. However, the CSA of connectors cannot be excessively enlarged, as this may reduce the embrasure space between the retainers and the pontic, thereby negatively impacting the esthetics of the restoration and increasing the difficulty of maintaining dental hygiene.

On the other hand, FPD materials may play a key role in determining stress distribution. Among various mechanical properties, elastic modulus is closely related, because it directly influences how a material responds to functional loads [10]. A higher elastic modulus allows the material to resist deformation, thereby transmitting forces more efficiently to the abutment teeth and surrounding tissues, while a lower elastic modulus may lead to greater flexibility, potentially reducing the stress on the supporting structures but increasing the risk of material fatigue or fracture [11]. Therefore, careful consideration of elastic modulus is essential for balancing durability and functional performance in FPDs. Herein, in the present

study, four materials with different elastic modulus were selected for investigation (zirconia [Zr], lithium disilicate [LD], polymer-infiltrated ceramic network [PICN], and resin composite [RC]) [12–15].

Stress analysis methodologies in biomechanical research typically involve both direct clinical evaluations and laboratory testing. Clinical evaluations are inherently limited by their inability to precisely quantify the stress distributed across specific components, such as the shoulder margin or the alveolar bone. Finite Element Analysis (FEA), on the other hand, offers distinct advantages over traditional methods, particularly in its ability to simulate and compute mechanical performance with a high degree of accuracy. FEA can effectively model the stress-strain relationships in structures with complex geometries and allow for detailed predictions of where stress concentrations occur and how they propagate through different materials or biological tissues [16]. Additionally, recent advancements in three-dimensional (3D) printing have further enhanced the application of stress analysis. 3D printed models can be used in photoelastic experiments to physically visualize the stress distribution. By combining the precision of FEA with the practical insights from photoelastic experiments, researchers can achieve a more robust understanding of mechanical performance in FPD-teeth-bone system.

To date, few studies have comprehensively investigated the effects of restorative materials and connector cross-section areas on the stress distribution in FPDs. To fill this scientific gap, four materials (Zr, LD, PICN, and RC) and five connector cross-section areas (4, 6, 8, 10, and 12 mm<sup>2</sup>) were chosen to examine the stress distribution in maxillary posterior fixed bridges using FEA. The results were further validated through photoelasticity experiments. It is important to note that the inclusion of these distinct materials aims to explore the biomechanical performance of FPDs as a function of varying elastic modulus, rather than to provide specific clinical recommendations for FPD material. The null hypotheses of this study were two-fold: (1) FPD materials do not influence on the stress distribution of FPDs, and (2) connector cross-section areas do not affect the stress distribution of FPDs.

## Methods

This study was approved by West China Hospital of Stomatology Ethics Committee (No. WCHSIRB-CT-2022-257). Digital Imaging and Communications in Medicine (DICOM) images of the upper jaw of a young female were obtained using cone-beam computed tomography (CBCT) (3D Accuitomo Type F17, Morita Corp., Japan), with a field view of  $\varnothing 40 \times h 40$  mm and a voxel size of 80  $\mu$ m. The first molar of the patient was intact, regular, and showed no signs of trauma or deformity.

Afterward, the DICOM data were imported into Solidworks software (Dassault Systèmes Solid Works® Corp., Concord, France) for 3D reconstruction. The first molar was then removed from the 3D model. Virtual tooth preparations were performed on the second premolar and second molar, following the requirements for all-ceramic monolithic crowns. Using commercial software (Materialise Magics, Materialise, Belgium), tooth reduction of 1.5 mm was applied to the occlusal surface and 1 mm to the axial surfaces, with the shoulder width set to 1 mm. FPDs were designed by commercially available software (Exocad 3.0, Exocad GmbH, Germany) and reverse engineering software (Geomagic Studio, 3D Systems Inc., USA), with a thickness of 1 mm at the cervical third, 1.5 mm at the occlusal third, and 1 mm at the middle third. The cement layer thickness was set to 0.03 mm [17], and the CSAs of connectors were designed at 4, 6, 8, 10, and 12 mm<sup>2</sup>. Afterward, FPDs and abutment teeth were assembled and imported to a finite element analysis software program (ANSYS Workbench 18.2.2, ANSYS Inc., USA) for load simulation (Fig. 1).

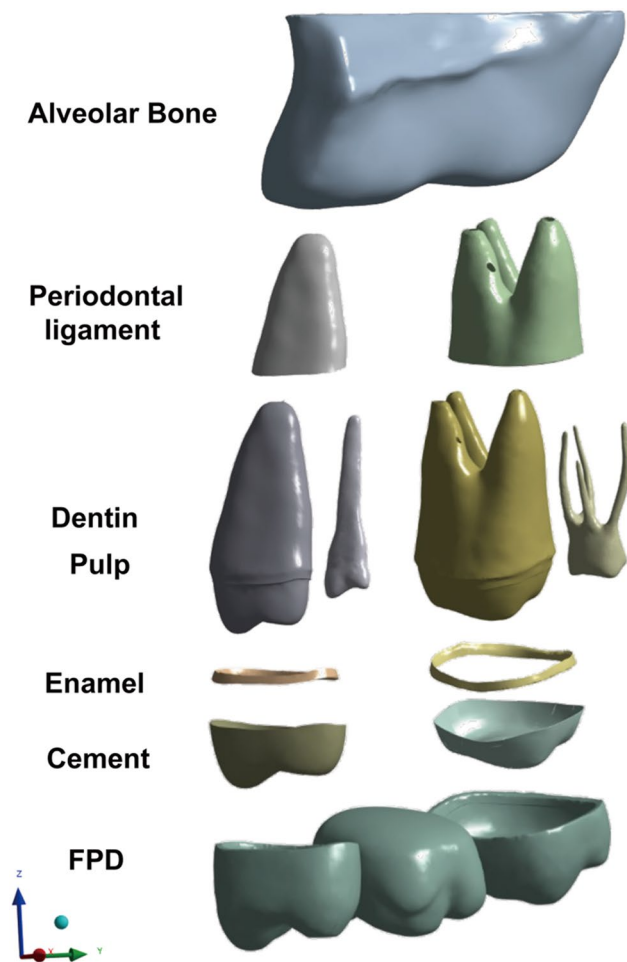


**Fig. 1** Components of the FPD-tooth-bone complex in three-dimensional finite element analysis

The elastic constants of the four investigated materials were extracted from previous literature and are summarized in Table S1 (Additional file 1). The materials were modeled as linearly elastic, homogeneous, and isotropic. All components were securely fixed within the coordinate system, with contact surfaces assumed to be fully bonded. The mesh size was set to 0.0002 mm, resulting in a total of 5,290,188 elements. The number of nodes was optimized to ensure model accuracy while minimizing computational load [18].

Two loading conditions were simulated to represent masticatory forces (Fig. 2) [19]. In the first condition (three-point loading), a vertical force of 200 N was applied to twelve 1 mm<sup>2</sup> areas on the occlusal surface of the FPD, simulating the chewing of large food blocks, where the loading areas were broad. In the second condition (pontic loading), a 200 N axial load was applied to three 1 mm<sup>2</sup> areas on the occlusal surface of the pontic, imitating the chewing of granular foods, where the loading areas were limited to the central groove region [20–22]. The von Mises stress distributions in the FPD, abutment teeth, periodontal ligament (PDL), and alveolar bone were analyzed, with both maximum principal stress and average values being calculated.

To further validate the results of FEA simulation, three typical CSA values (4, 8, and 12 mm<sup>2</sup>) and two materials (Zr and RC) were selected for investigation in a photoelastic experiment as previously reported [23]. In brief, six pairs of natural teeth (#15 and #17) with similar shape and size were scanned to generate Standard Tessellation Language (STL) files, which were then virtually positioned into the maxillary alveolar bone model 3D reconstructed in FEA. The root surfaces of teeth #15 and #17 were expanded outward by 0.2 mm to create space for the PDL [24]. Afterward, a Boolean operation was conducted to subtract intact teeth #15 and #17 from the maxilla. The obtained alveolar models were then 3D printed using a Digital Light Processing (DLP) 3D printer (3Dmax, DMG Medical Devices Co. Ltd., Germany). Next, negative molds of the 3D printed molds were prepared by silicone rubber, and a photoelastic resin (epoxy resin, JN-L, China) was poured to create the photoelastic model. Before the photoelastic model fully cured, light-body silicone rubber was injected into the sockets to simulate a 0.2 mm thick PDL, and the corresponding teeth #15 and #17 were inserted into the photoelastic model. Afterward, the abutment teeth (#15 and #17) were prepared by the same prosthodontist and 3D scanned. Three-unit FPDs were designed with the three different CSA values, and then produced by a milling device (Upcera X5, Upcera, China) using Zr (98\*14-A2, Batch B2824020901, Besmile, China) and RC (98\*18-2M2, Batch HL22070401, Huliang, China). To ensure structural consistency, the thickness of the shoulder, axial surface, and occlusal

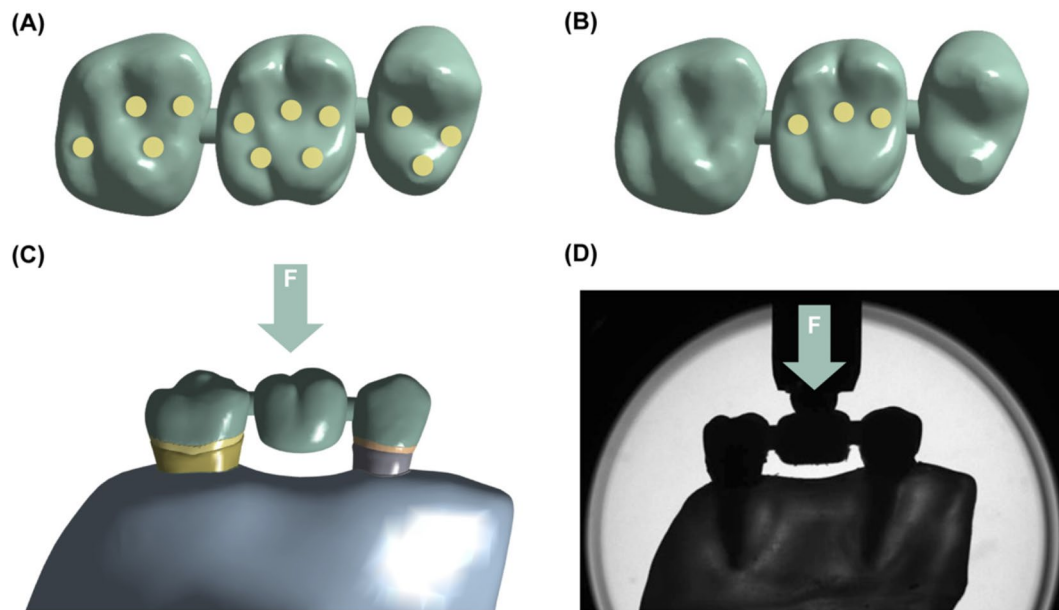


**Fig. 2** Schematic diagrams of two loading modes on FPDs in the three-dimensional finite element analysis. The upper diagrams show the loading areas on the occlusal surfaces of FPDs under (A) three-point loading and (B) pontic loading. Yellow dots represent loading areas of  $1\text{ mm}^2$ . A vertical load of 200 N was applied to the FPD in both (C) finite element analysis and (D) photoelastic analysis

surface was 1 mm, 1 mm, and 1.5 mm, respectively. The connector was cylindrical in shape. After cementing the FPDs onto the abutment teeth using resin cement (3M ESPE Rely™ U200 Automix, 3M ESPE, USA), the final test sample for photoelastic experiment was prepared. Each sample was horizontally placed in a polarized light field, and a vertical load of 200 N was applied to the pontic using a universal test machine (AGX-V, SHIMADZU, Japan), with the load cell aligned with the center of the pontic's central fossa. The change in the refraction path of polarized light, observed before and after loading, was used to calculate the equivalent stress. A mathematical analysis software (Matlab\_R 2023a, The MathWorks, Inc., USA) was used for plotting stress distribution.

## Results

FPD material showed a significant effect on the stress distribution in the FPDs, abutment teeth, PDL and alveolar bone. For both maximum and average stress levels in FPD, Zr exhibited the highest values, followed by LD, PICN, and RC (Fig. 3A and B). In contrast to the FPD ranking, the average stress on abutment teeth was the highest in RC group, followed by PICN, LD, and Zr (Fig. 3D). For instance, with a CSA of  $8\text{ mm}^2$ , the average stress in the FPD gradually decreased, while the stress in the abutment teeth increased, following the material order: Zr (8.7071 MPa, 2.4177 MPa), LD (8.0162 MPa, 2.4750 MPa), PICN (6.7848 MPa, 2.6031 MPa), and RC (5.8681 MPa, 2.7359 MPa). The maximum stress of abutment in RC was higher than the one in PICN, with

increases of 12.95% at  $10\text{ mm}^2$  and 101.45% at  $12\text{ mm}^2$  CSA (Fig. 3C).

In terms of periodontal tissues (Figs. 4 and 5), the average stress in the PDL at  $12\text{ mm}^2$  CSA was 1.2807 MPa in Zr, followed by LD (1.2796 MPa, -0.09%), PICN (1.2778 MPa, -0.23%), and RC (1.2760 MPa, -0.37%) (Fig. 3E).

Despite differences in the stress levels within the periodontal tissues, the PICN group showed minimal fluctuations in the average PDL stress under pontic loading, with changes of less than 0.04% (Fig. 6D). Regarding stress concentration sites, the connectors and loading points on the occlusal surfaces of the FPDs were the most prominent (Figs. 7 and 8).

High-stress areas on the abutments, ranging from 6.25 to 31.25 MPa, were observed on the shoulder and proximal surfaces near the pontic. However, in the RC and PICN groups, the proximal surfaces exhibited larger regions with stress exceeding 25 MPa, and in the RC group, the stress at the shoulder surpassed 50 MPa (Fig. 9).

CSA was negatively correlated with the stress levels in both the FPD and abutment teeth, while it exhibited a positive correlation with the stress levels in the PDL and alveolar bone. In the Zr group, the average stress in the FPD was 9.2075 MPa for a CSA of  $4\text{ mm}^2$ , 8.9262 MPa for  $6\text{ mm}^2$ , 8.7071 MPa for  $8\text{ mm}^2$ , 8.5847 MPa for  $10\text{ mm}^2$ , and 8.5192 MPa for  $12\text{ mm}^2$ . This reflects a gradual reduction of 3.06%, 5.43%, 6.76%, and 7.48%, respectively, as the CSA increased. Similar decreasing trends could also be observed in the LD, PICN, and RC groups

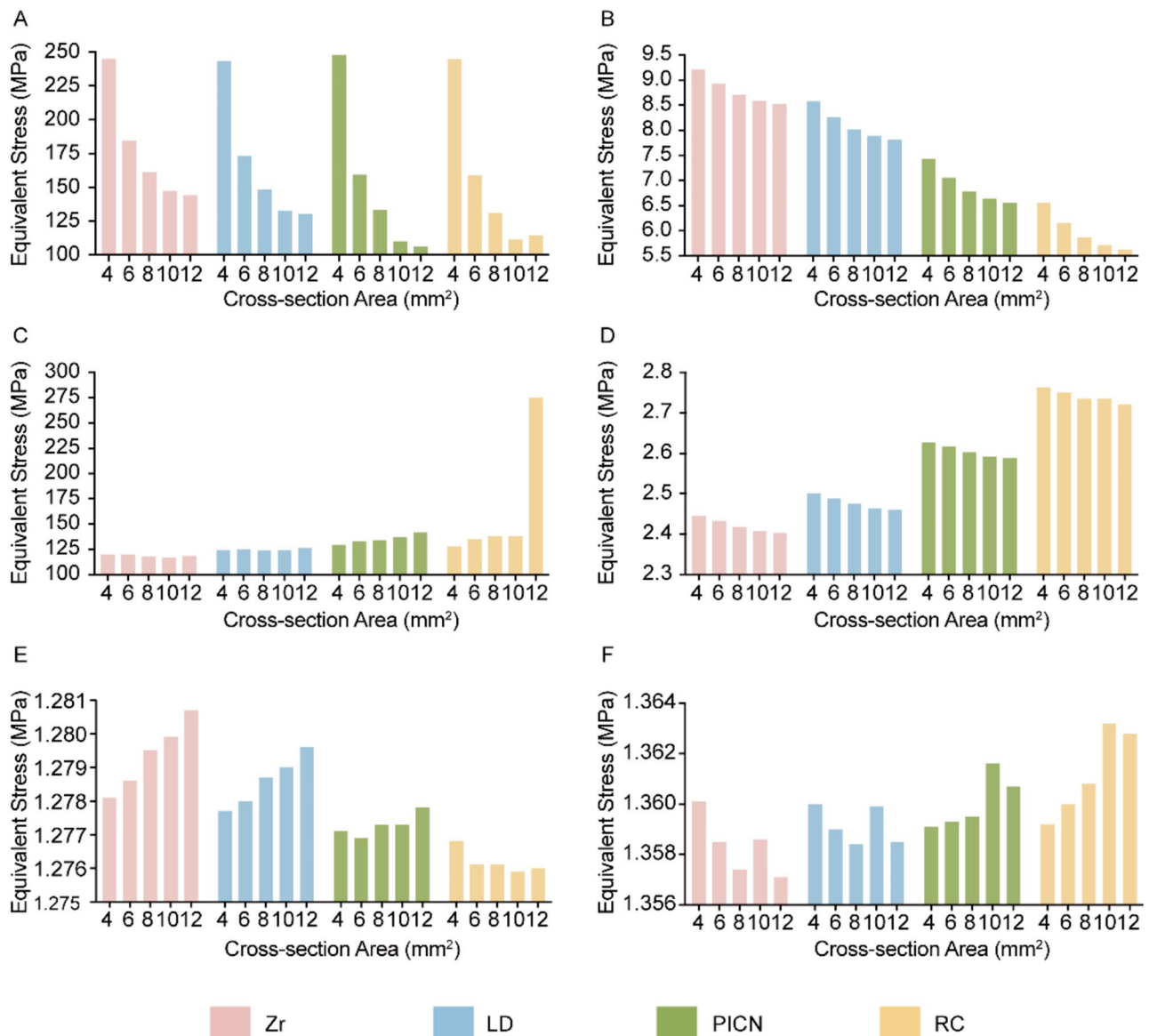


**Fig. 3** The equivalent stress (MPa) of 3D FEA models under three-point loading. **(A)** Maximum and **(B)** average stress on fixed partial dentures. **(C)** Maximum and **(D)** average stress on abutment teeth. **(E)** Average stress on periodontal ligament. **(F)** Average stress on alveolar bone

(Fig. 3B). For abutment teeth in the Zr group, the average stress was the highest at 4 mm<sup>2</sup> CSA (2.433 MPa), followed by a decrease to 2.4318 MPa (-0.46%) at 6 mm<sup>2</sup>, 2.4177 MPa (-1.04%) at 8 mm<sup>2</sup>, 2.4074 MPa (-1.46%) at 10 mm<sup>2</sup>, and 2.4033 MPa (-1.63%) at 12 mm<sup>2</sup>, showing a consistent decline as CSA increased. This declining trend was consistent across the Zr, PICN, and RC groups (Fig. 3D). However, in the PICN group, the maximum stress in the abutment teeth increased by 9.47% as the CSA increased from 4 mm<sup>2</sup> to 12 mm<sup>2</sup>. Moreover, in the RC group, the maximum stress in the abutment teeth increased by 5.84%, 8.29%, 34.70%, and 115.63% at CSAs of 6 mm<sup>2</sup>, 8 mm<sup>2</sup>, 10 mm<sup>2</sup>, and 12 mm<sup>2</sup>, respectively, compared to that at the CSA of 4 mm<sup>2</sup> (Fig. 3C).

The stress distribution at the cross-section between the connector and retainer exhibited a “C” shape, likely due to the occlusal contact point being set towards the buccal side of the central groove. Additionally, the area with stress exceeding 50 MPa decreased in size as the CSA increased (Fig. 10).

The stress distribution under pontic loading was largely consistent with that observed under three-point loading (Figs. 11 and 12). However, irregular trends were noted in the LD group at a CSA of 10 mm<sup>2</sup>, the RC group at 12 mm<sup>2</sup>, and the Zr group at 8 mm<sup>2</sup> (Figs. 6 and 13).

As shown in Fig. 14, the photoelasticity results indicated that, for the same CSA, the area with high equivalent stress (>150) was larger in the RC group compared

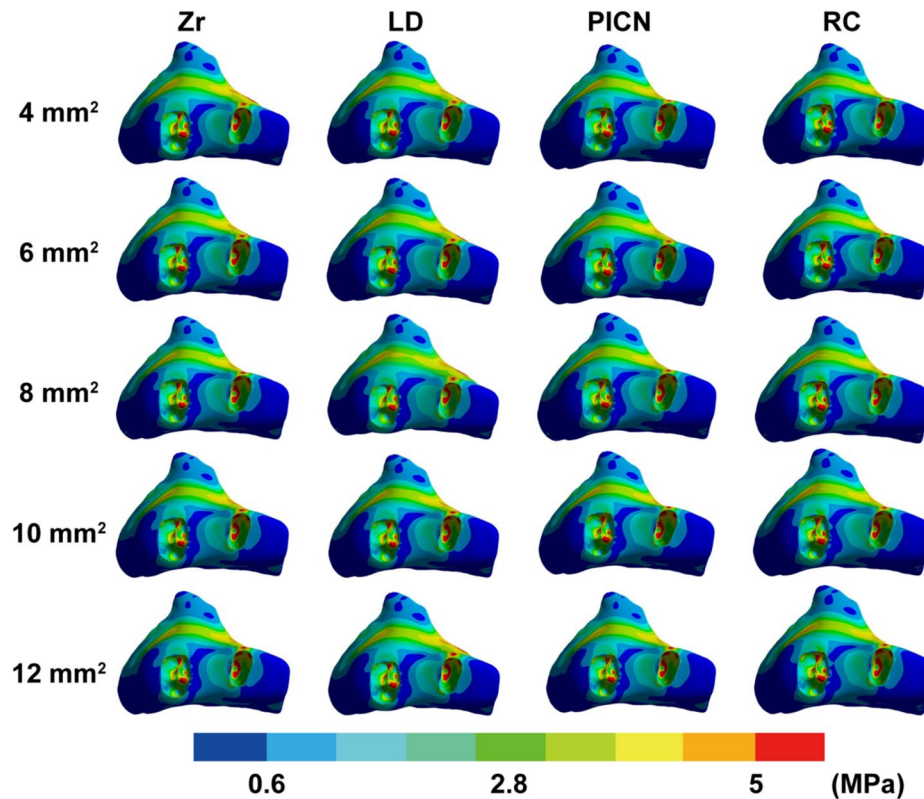


**Fig. 4** Stress distribution under three-point loading on alveolar bone. The cross-section areas of the connectors are listed on the left

to the Zr group. For the same FPD material, the equivalent stress levels declined as the CSA increased. These photoelastic findings were consistent with the FEA results (Figs. 4 and 5).

## Discussion

The stress distribution in the FPD-tooth-bone complex follows a predictable pattern where occlusal forces are transmitted from the prosthesis to the abutment teeth, and then to the underlying PDL and alveolar bone. Studies have reported that the 10-year survival rate of monolithic lithium disilicate FPDs is 87.9% [25], while the 5-year survival rates for reinforced glass-ceramic FPDs and densely sintered zirconia FPDs are 85.9% and 90.4%, respectively. FPD fracture and periodontal disease are among the primary causes of failure [26]. Therefore, achieving proper stress distribution is essential to prevent overloading of any single component, thereby ensuring the longevity of the restoration and preserving the supporting structures.

The results of this study demonstrate that both FPD materials and connector cross-section areas affect the stress distribution of FPDs. Therefore, both null hypotheses were rejected. Specifically, the stress experienced by the FPD is positively correlated with the elastic modulus of the FPD material, whereas the stress on the abutment teeth exhibits an opposite trend (Fig. 3A and D). Due to

the high elastic modulus of Zr and LD [12, 13], stress can be more effectively distributed across the FPD, thereby reducing the load on the abutment teeth and providing effective protection to the surrounding tissues. However, this effect may also lead to an increase in tensile stress within the FPD, therefore, FPD materials with high elastic modulus should also possess sufficient fracture toughness to prevent FPD fracture [27]. Compared to Zr and LD, PICN possesses a moderate elastic modulus, which lies between that of enamel and dentin [14]. This results in a reduction of stress borne by the FPD and a greater stress distributed to the abutment teeth, while the stress on the PDL remains almost unchanged (Figs. 3A and D and 6D). Among the four materials studied, RC exhibits the lowest elastic modulus [28]. Compared to the other three groups, the RC group exhibited less stress on the FPD, while the abutment teeth were subjected to higher stress. Notably, when the CSA reached 12 mm<sup>2</sup>, significant stress concentration was observed on the abutment teeth (Fig. 3A and D). When comparing all-ceramic materials (Zr and LD) with composite materials (PICN and RC), it was observed that the maximum stress on the FPD in the Zr and LD groups consistently exceeded that on the abutment teeth. However, in the PICN and RC groups, when the CSA was 8, 10, or 12 mm<sup>2</sup>, the maximum stress on the abutment teeth surpassed that on the FPD, with the stress on the abutment teeth primarily concentrated

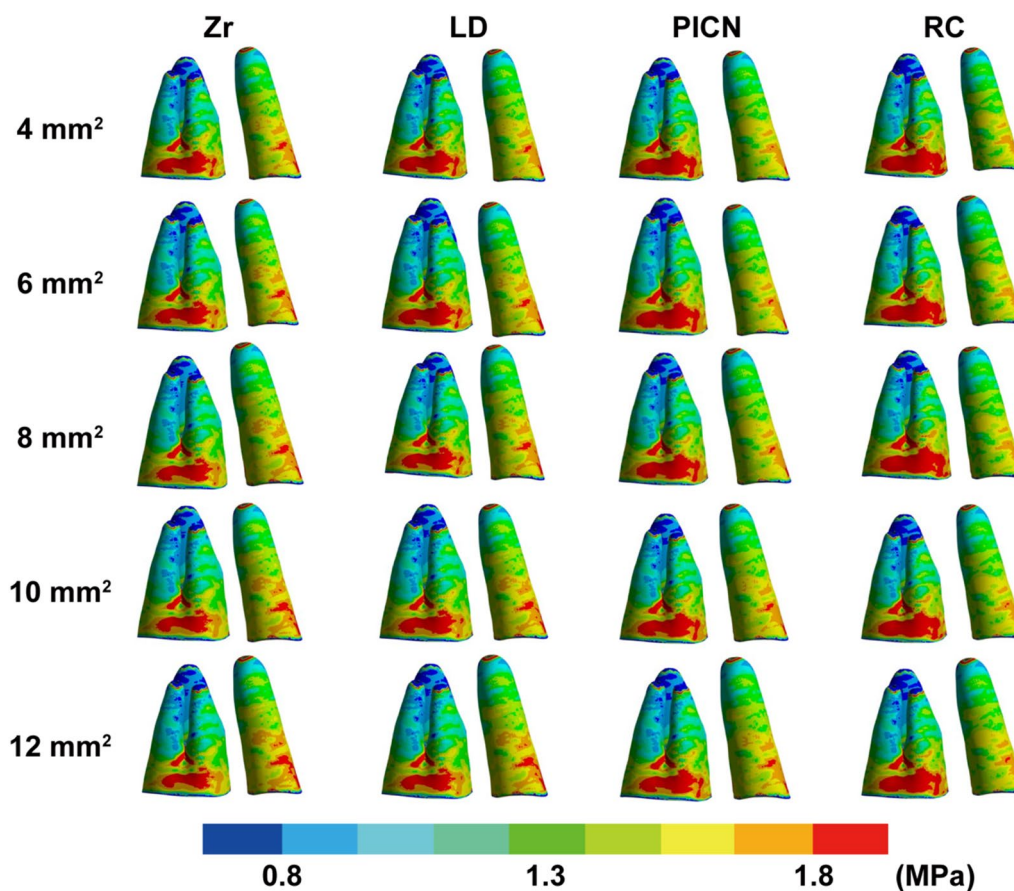


**Fig. 5** Stress distribution under three-point loading on periodontal ligaments. The cross-section areas of the connectors are listed on the left

at the shoulder margin (Figs. 3A and C and 8). Furthermore, in periodontal tissues, as the CSA increased, the Zr and LD groups primarily exhibited a gradual increase of stress in PDL (Fig. 3E), whereas the PICN and RC groups showed an increasing stress in alveolar bone (Fig. 3F). This difference may be related to the varying extent of stress transmission downward. With higher rigidity, Zr and LD exhibit less deformation under load, causing stress to be primarily concentrated within the FPD, with less stress transmitted downward. The stress transmitted to the PDL can be buffered and absorbed effectively. In contrast, due to the lower stiffness, PICN and RC may undergo greater deformation when subjected to force, leading to more stress being transmitted downward to the alveolar bone. In general, the results suggest that the decrease in elastic modulus of FPD material may weaken the protective effect of the FPD on the abutment teeth, increasing the risk of marginal infiltration, adhesive failure, periodontal damage, and even bone resorption, especially when the CSA is relatively large [29].

The stress on both the FPD and abutment teeth were found to be negatively correlated with the CSA (Fig. 3A and D). A smaller CSA tends to concentrate stress within the FPD, particularly in the connector region, resulting in

less stress being distributed to the abutment teeth (Figs. 7 and 8). This might be because a larger CSA allows for a more uniform distribution of stress. However, once the CSA reaches a certain size, further increases in CSA do not significantly reduce the stress on the FPD and abutment teeth (Fig. 3B, D). Additionally, an excessively large CSA may lead to the reduction of the embrasure space, affecting the aesthetics of the FPD. It may also lead to the formation of overcontours, which can hinder oral hygiene and compromise the health of gingival tissues. The results of this study indicate that the connectors and occlusal loading areas are the primary sites of stress concentration, with the magnitude of stress concentration being positively correlated with the elastic modulus of the FPD material (Fig. 8). This finding aligns with previous research by Attia et al., which identified the connector (particularly at the gingival embrasure) as prone to stress concentration and rupture [30]. Additionally, it supports the conclusions of Tribst et al., who demonstrated that the degree of stress concentration is proportional to the elastic modulus of the FPD material [31]. Considering the discrepancies between computational simulations and clinical realities, we further validated the finite element analysis results using real models. Photoelastic

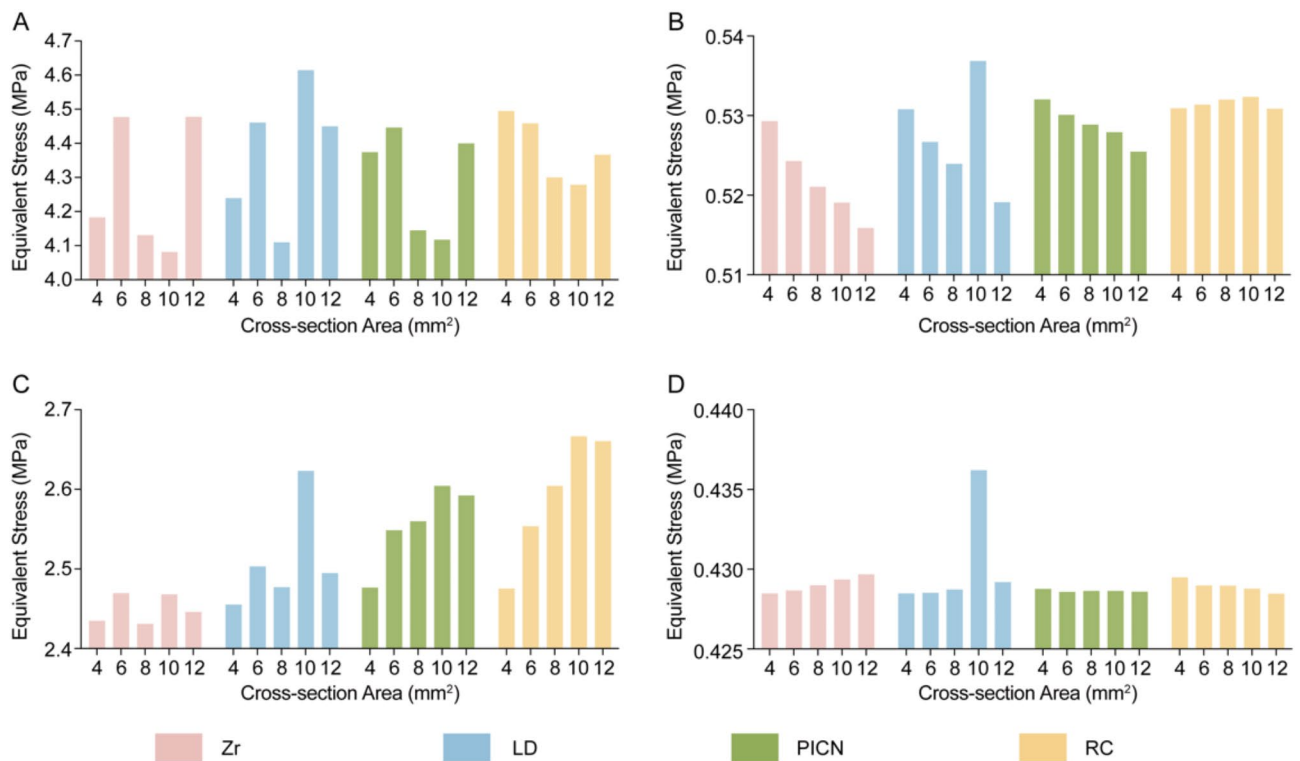


**Fig. 6** Equivalent stress (MPa) of 3D FEA models under pontic loading. (A) Maximum and (B) average stress on alveolar bone. (C) Maximum and (D) average stress on periodontal ligament

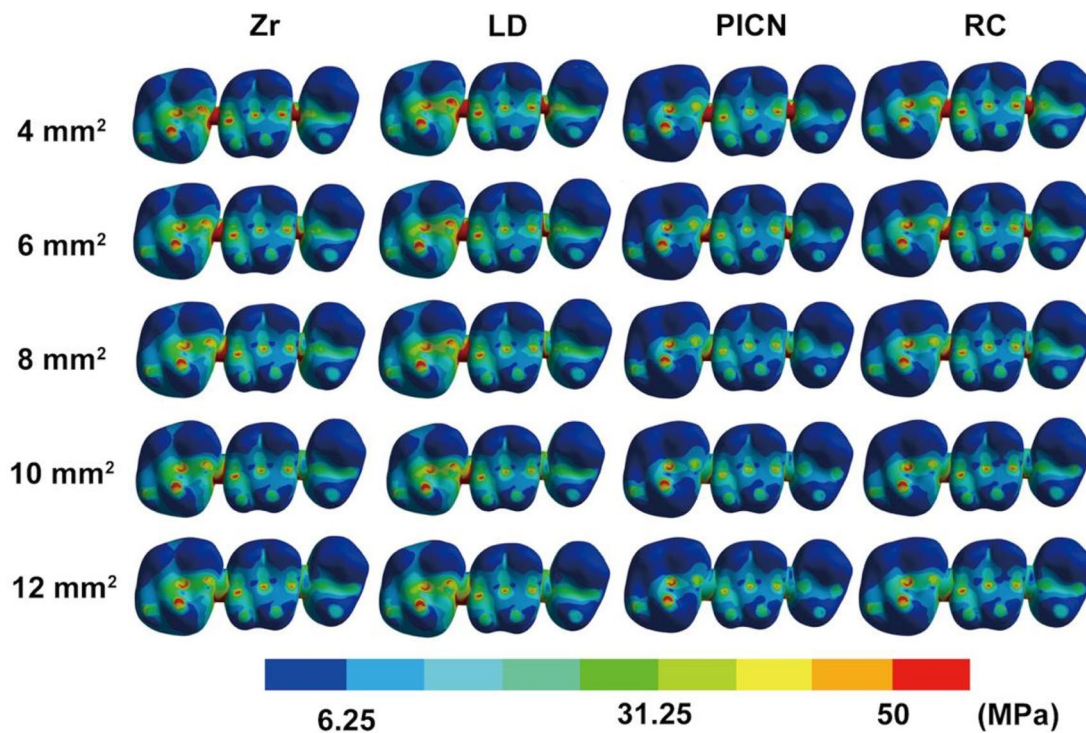


**Fig. 7** The stress distribution under the three-point loading on the occlusal surface of FPDs. The cross-section areas of the connectors are listed on the left

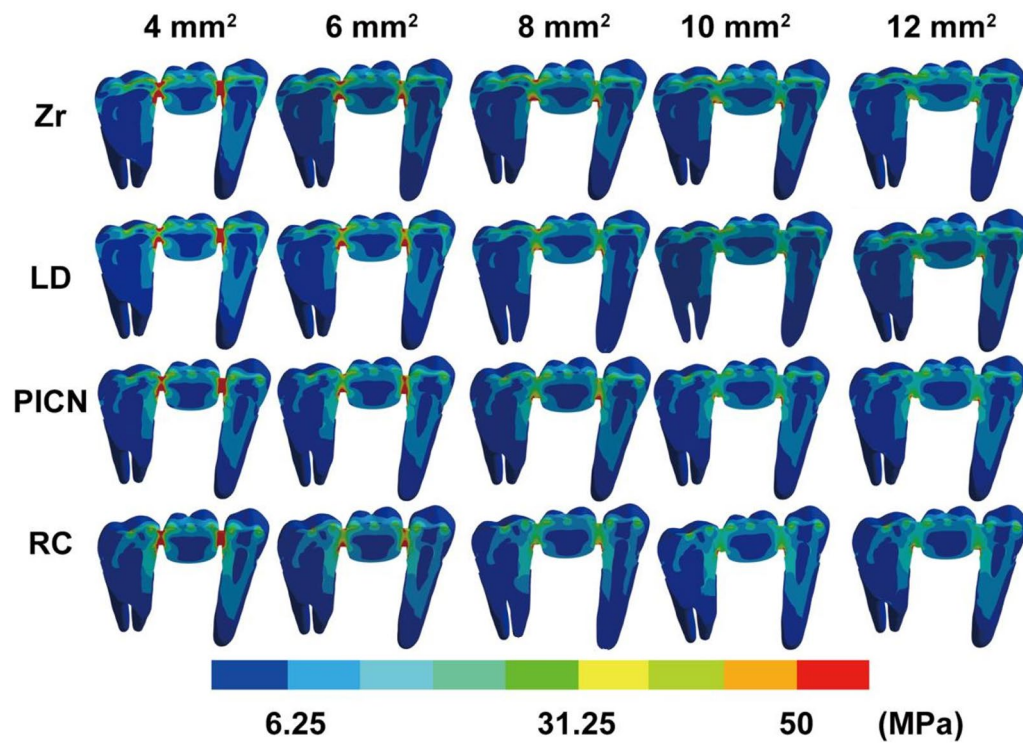


**Fig. 8** Stress distribution under three-point loading on median sagittal plane of FPDs. The cross-section areas of the connectors are labelled on the top

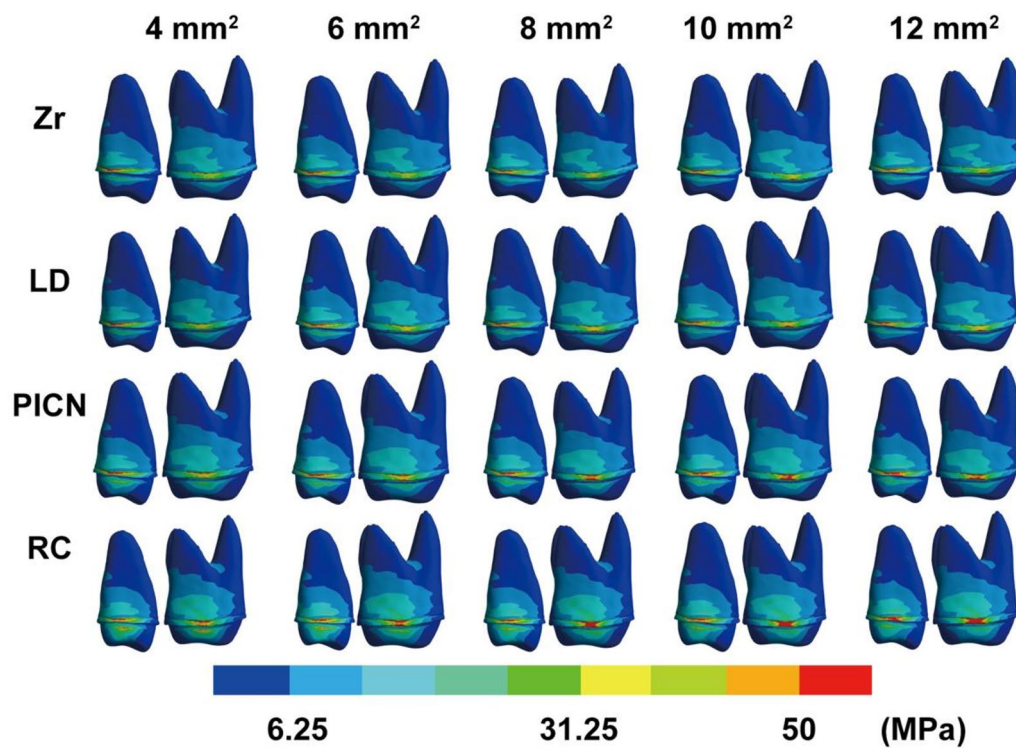


**Fig. 9** Stress distribution under three-point loading on abutment teeth #15 (distal) and #17 (mesial). The cross-section areas of the connectors are labelled on the top

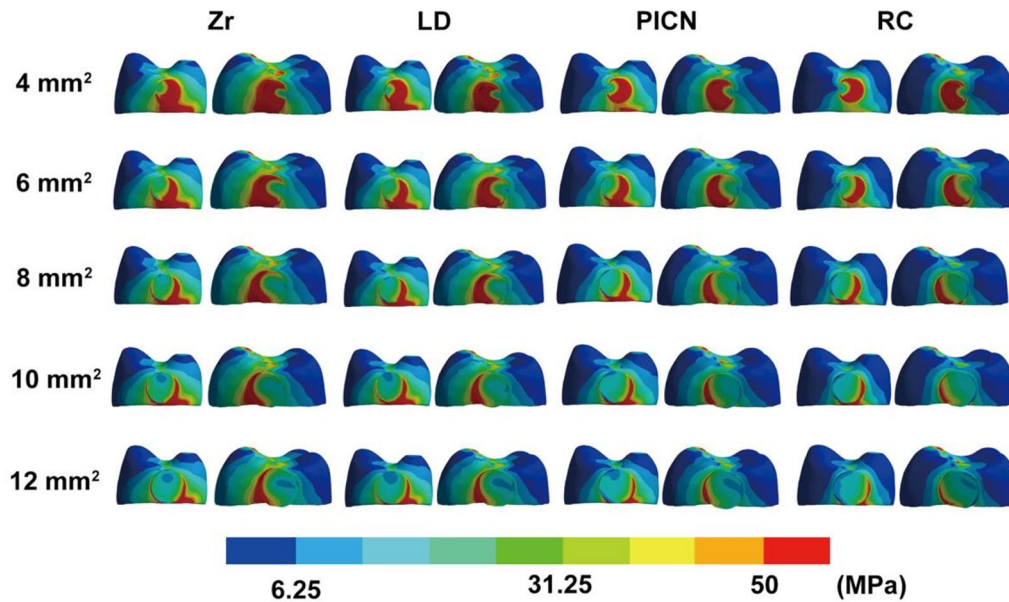


**Fig. 10** The stress distribution under three-point loading between connectors and retainers. The cross-section areas of the connectors are labelled on the left

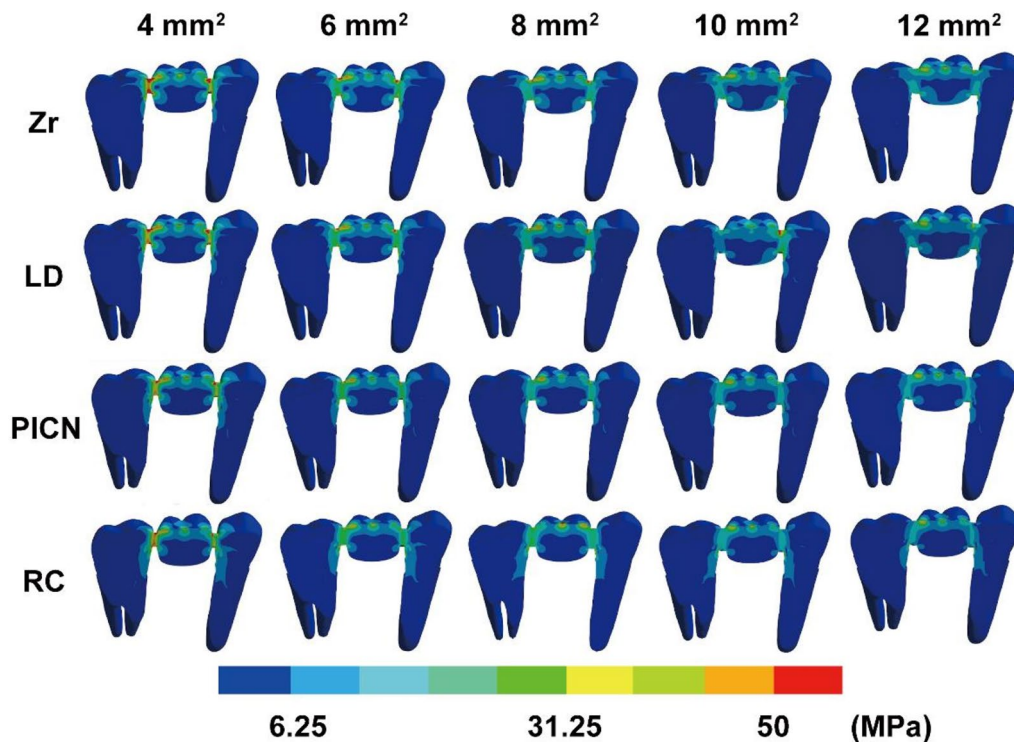


**Fig. 11** Stress distribution under pontic loading on median sagittal plane of FPDs. The cross-section areas of the connectors are labelled on the top

analysis and strain gauge methods are classic stress analysis techniques [32]. Among these, photoelastic analysis offers the advantage of not requiring direct contact with the sample, making it suitable for models where components, such as the PDL, alveolar bone, and tooth root, are in close contact. Unlike traditional methods, 3D printing

was employed in this study to fabricate models for photoelastic testing due to its superior reproducibility in mass production of test samples. However, the accuracy of this workflow warrants further research for a full revelation. The results of photoelastic experiment were presented as the ratio of the optical path difference. Although this

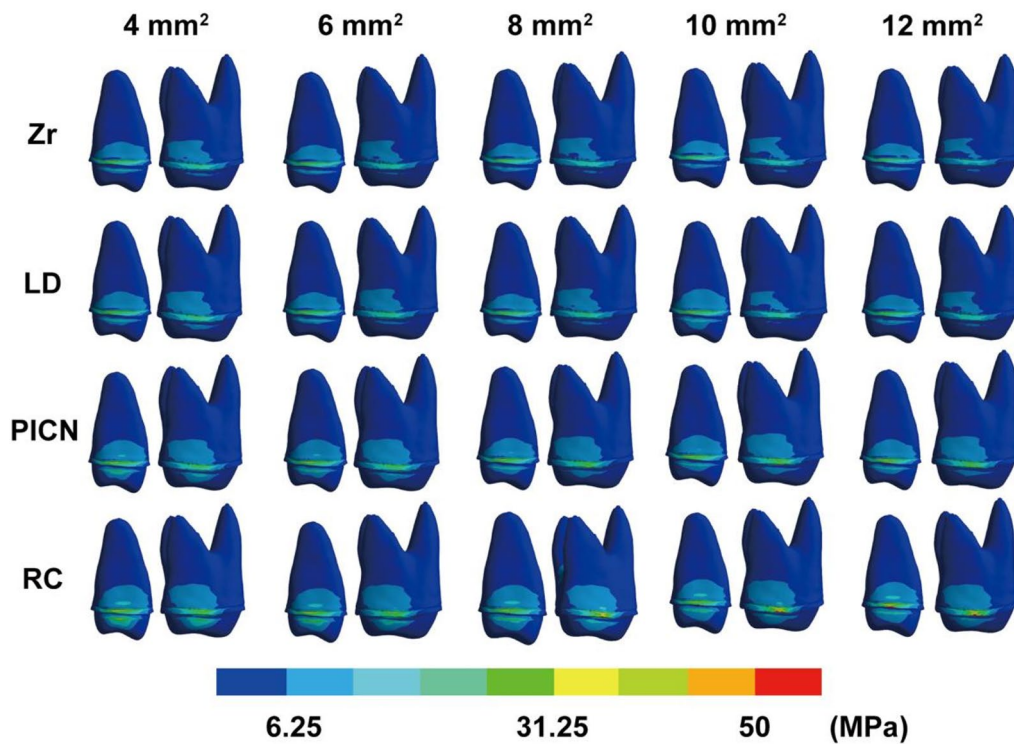


**Fig. 12** Stress distribution under pontic loading on abutment teeth #15 (distal) and #17 (mesial). The cross-section areas of the connectors are labelled on the top

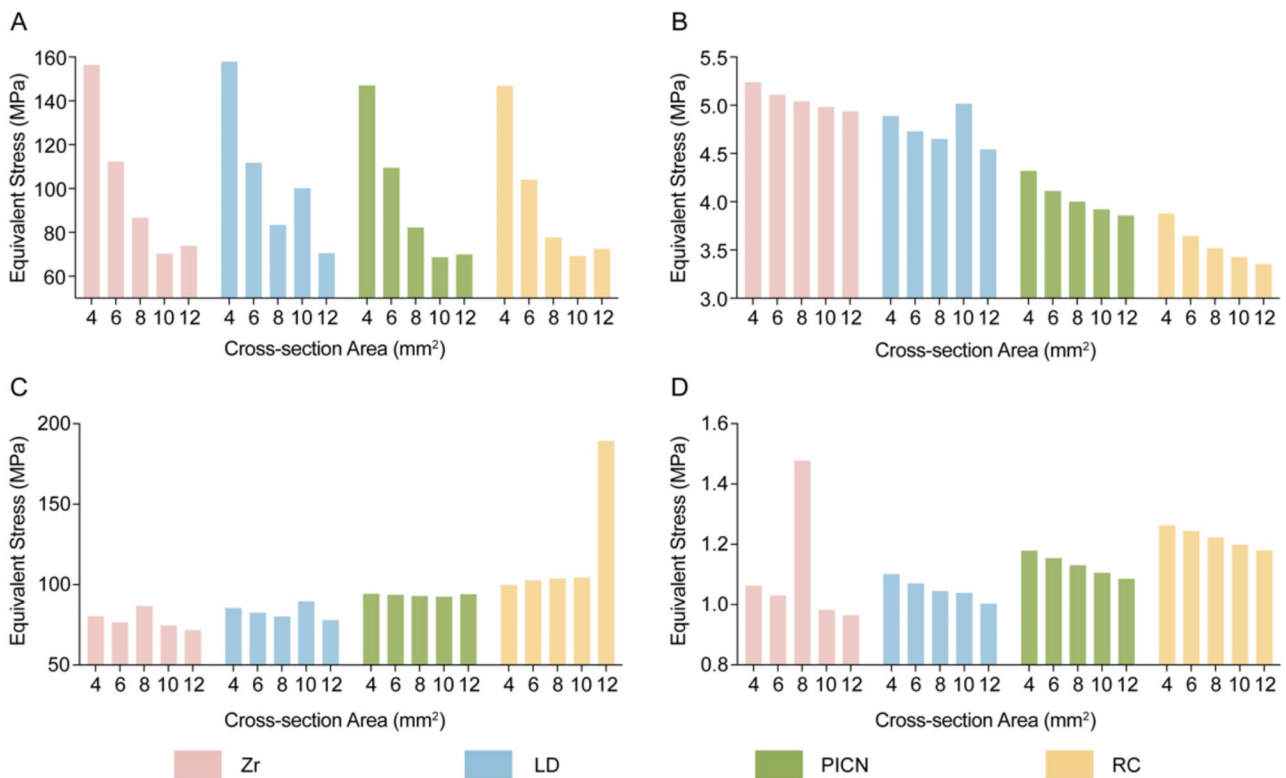


**Fig. 13** Equivalent stress (MPa) of 3D FEA models under pontic loading. (A) Maximum and (B) average stress on fixed partial dentures. (C) Maximum and (D) average stress on abutment teeth

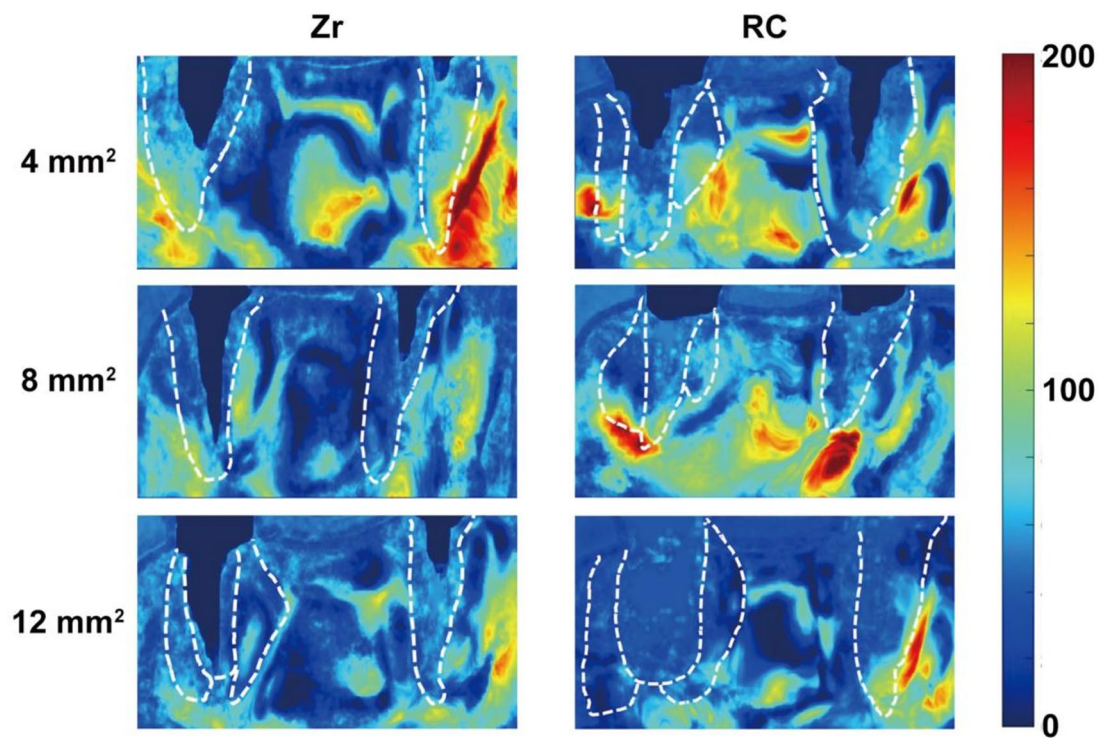


**Fig. 14** Photoelastic analysis of stress distribution under 200 N axial loading on the pontic. The cross-section areas of the connectors are labelled on the left. The color bar on the right indicates equivalent stress (arbitrary units)

is equivalent to stress values, the present study is limited in calculating absolute values. Future research may address this limitation by integrating digital image correlation (DIC) for more accurate quantitative analysis. The FEA analysis in this study focused on Von Mises stress because PICN, RC, dentin, PDL, and alveolar bone exhibit varying degrees of ductility. However, the maximum principal stress is also worth investigating in future studies because it plays a crucial role in evaluating the fracture risk and failure mechanism of brittle materials. Moreover, another limitation of this study is the absence of setting a fulcrum point for the tooth roots under pontic loading in FEA. Although the deformation of FPDs and the rotation of abutment teeth are minimal, setting such a fulcrum point could enable a more accurate analysis of the stress distribution within the support system. This study provides potential insights into the design and material selection for FPDs. The results suggest that materials with a high elastic modulus may require an increased CSA to distribute stress evenly and reduce the stress borne by the FPD. Conversely, for materials with a low elastic modulus, the CSA should be reduced to avoid excessive stress on periodontium.

## Conclusion

Our findings indicate that materials with a higher elastic modulus tend to confine stress within the FPDs, thereby transmitting less stress to the abutment teeth. While this

effect may protect the underlying supportive tissues, it simultaneously increases the stress borne by FPD. Moreover, as the CSA increases, stress might be more evenly transferred from FPD to the supporting structures, potentially reducing stress concentration. However, excessively increasing the CSA does not further lower stress levels on the FPD and abutment teeth, but may negatively impact aesthetics.

## Abbreviations

CSA	Cross-section area
FPD	Fixed partial denture
Zr	Zirconia
LD	Lithium Disilicate
PICN	Polymer-infiltrated ceramic network
RC	Resin composite
FEA	Finite element analysis
PDL	Periodontal ligament
3Y-TZP	3 mol% yttria-stabilized tetragonal zirconia polycrystals
3D	Three-dimensional
DICOM	Digital Imaging and Communications in Medicine
CBCT	Cone-beam computed tomography
STL	Standard Tessellation Language
DLP	Digital Light Processing

## Supplementary Information

The online version contains supplementary material available at <https://doi.org/10.1186/s13005-025-00484-y>.

Supplementary Material 1

**Acknowledgements**

Not applicable.

**Author contributions**

J.C., T.Z. and R.L. conducted investigations and experiments. J.C. and Y.X. wrote the main manuscript. J.C. and T.Z. prepared all figures and the table. Z.Z. and X.P. handled data curation, reviewing and editing. Y.X. and Q.W. participated in conceptualization. All authors reviewed the manuscript.

**Funding**

This work was supported by the National Key Research and Development Program of China (No. 2022YFC2410103).

**Data availability**

No datasets were generated or analysed during the current study.

**Declarations****Ethics approval and consent to participate**

This study was approved by West China Hospital of Stomatology Ethics Committee (No. WCHSIRB-CT-2022-257).

**Consent for publication**

Not applicable.

**Competing interests**

The authors declare no competing interests.

Received: 24 October 2024 / Accepted: 3 February 2025

Published online: 28 February 2025

**References**

- Heintze SD, Monreal D, Reinhardt M, Eser A, Peschke A, Reinshagen J, et al. Fatigue resistance of all-ceramic fixed partial dentures - fatigue tests and finite element analysis. *Dent Mater.* 2018;34(3):494–507.
- Mazza LC, Lemos CAA, Pesqueira AA, Pellizzer EP. Survival and complications of monolithic ceramic for tooth-supported fixed dental prostheses: a systematic review and meta-analysis. *J Prosthet Dent.* 2022;128(4):566–74.
- Oh W, Götzén N, Anusavice KJ. Influence of connector design on fracture probability of ceramic fixed-partial dentures. *J Dent Res.* 2002;81(9):623–7.
- Ramakrishaniah R, Al Kheraif AA, Elsharawy MA, Alsaleh AK, Ismail Mohamed KM, Rehman IU. A comparative finite elemental analysis of glass abutment supported and unsupported cantilever fixed partial denture. *Dent Mater.* 2015;31(5):514–21.
- Valera-Jiménez JF, Burgueño-Barris G, Gómez-González S, López-López J, Valmaseda-Castellón E, Fernández-Aguado E. Finite element analysis of narrow dental implants. *Dent Mater.* 2020;36(7):927–35.
- Larsson C, Holm L, Lövgren N, Kokubo Y, Vult von Steyern P. Fracture strength of four-unit Y-TZP FPD cores designed with varying connector diameter. An in-vitro study. *J Oral Rehabil.* 2007;34(9):702–9.
- Stuart AR, Filser F, Kocher P, Lüthy H, Gauckler LJ. Cyclic fatigue in water of veneer-framework composites for all-ceramic dental bridges. *Dent Mater.* 2007;23(2):177–85.
- Schmitter M, MUSSOTTER K, RAMELSBERG P, STOBER T, GABBERT OHL-MANNB. Clinical performance of extended zirconia frameworks for fixed dental prostheses: two-year results. *J Oral Rehabil.* 2009;36(8):610–5.
- Stuart AR, Filser F, Kocher P, Gauckler LJ. Fatigue of zirconia under cyclic loading in water and its implications for the design of dental bridges. *Dent Mater.* 2007;23(1):106–14.
- Tribst JPM, Dal Piva AMO, Madruga CFL, Valera MC, Borges ALS, Bresciani E, et al. Endocrown restorations: influence of dental remnant and restorative material on stress distribution. *Dent Mater.* 2018;34(10):1466–73.
- Dal Piva AMO, Tribst JPM, Borges ALS, Souza RODAe, Bottino MA. CAD-FEA modeling and analysis of different full crown monolithic restorations. *Dent Mater.* 2018;34(9):1342–50.
- Zhang Y, Lawn BR. Novel zirconia materials in Dentistry. *J Dent Res.* 2018;97(2):140–7.
- Spitznagel F, Boldt J, Giethmuehlen P. CAD/CAM ceramic restorative materials for natural teeth. *J Dent Res.* 2018;97(10):1082–91.
- Swain MV, Coldea A, Bilkhair A, Guess PC. Interpenetrating network ceramic-resin composite dental restorative materials. *Dent Mater.* 2016;32(1):34–42.
- Alp G, Murat S, Yilmaz B. Comparison of Flexural Strength of different CAD/CAM PMMA-Based polymers. *J Prosthodont.* 2019;28(2):e491–5.
- Yoda N, Liao Z, Chen J, Sasaki K, Swain M, Li Q. Role of implant configurations supporting three-unit fixed partial denture on mandibular bone response: biological-data-based finite element study. *J Oral Rehabil.* 2016;43(9):692–701.
- Torcato LB, Pellizzer EP, Verri FR, Falcón-Antenucci RM, Santiago Júnior JF, de Faria Almeida DA. Influence of parafunctional loading and prosthetic connection on stress distribution: a 3D finite element analysis. *J Prosthet Dent.* 2015;114(5):644–51.
- Li R, Wu Z, Chen S, Li X, Wan Q, Xie G, et al. Biomechanical behavior analysis of four types of short implants with different placement depths using the finite element method. *J Prosthet Dent.* 2023;129(3):447.e1–e10.
- Ferrario VF, Sforza C, Serrao G, Dellavia C, Tartaglia GM. Single tooth bite forces in healthy young adults. *J Oral Rehabil.* 2004;31(1):18–22.
- Wu W, Song L, Liu J, Du L, Zhang Y, Chen Y, et al. Finite element analysis of the angle range in trans-inferior alveolar nerve implantation at the mandibular second molar. *BMC Oral Health.* 2023;23(1):928.
- Yoon HG, Oh HK, Lee DY, Shin JH. 3-D finite element analysis of the effects of post location and loading location on stress distribution in root canals of the mandibular 1st molar. *J Appl Oral Sci.* 2018;26:e20160406.
- de la Rosa Castolo G, Guevara Perez SV, Arnoux PJ, Badih L, Bonnet F, Behr M. Implant-supported overdentures with different clinical configurations: mechanical resistance using a numerical approach. *J Prosthet Dent.* 2019;121(3):546.e1–e10.
- Zhu T, Chen J, Xu Y, Zhu Z, Wang J, Pei X, et al. Biomechanical behaviour of tilted abutment after fixed partial denture restoration of CAD/CAM materials. *BMC Oral Health.* 2024;24(1):1128.
- Ozcelik T, Ersoy AE. An investigation of tooth/implant-supported fixed prosthesis designs with two different stress analysis methods: an in vitro study. *J Prosthodont.* 2007;16(2):107–16.
- Kern M, Sasse M, Wolfart S. Ten-year outcome of three-unit fixed dental prostheses made from monolithic lithium disilicate ceramic. *J Am Dent Assoc.* 2012;143(3):234–40.
- Pjetursson BE, Sailer I, Makarov NA, Zwahlen M, Thoma DS. All-ceramic or metal-ceramic tooth-supported fixed dental prostheses (FDPs)? A systematic review of the survival and complication rates. Part II: multiple-unit FDPs. *Dent Mater.* 2015;31(6):624–39.
- Juloski J, Apicella D, Ferrari M. The effect of ferrule height on stress distribution within a tooth restored with fibre posts and ceramic crown: a finite element analysis. *Dent Mater.* 2014;30(12):1304–15.
- Zafar MS. Prosthodontic applications of Polymethyl Methacrylate (PMMA): an update. *Polym (Basel).* 2020;12(10).
- Campaner LM, Silveira MPM, de Andrade GS, Borges ALS, Bottino MA, Dal Piva AMO, et al. Influence of polymeric restorative materials on the stress distribution in posterior fixed partial dentures: 3D finite element analysis. *Polym (Basel).* 2021;13(5):758.
- Attia MA, Shokry TE. Effect of dynamic loading on fracture resistance of gradient zirconia fixed partial denture frameworks. *J Prosthet Dent.* 2023;130(2):242–9.
- Tribst JPM, Dal Piva AMO, de Melo RM, Borges ALS, Bottino MA, Özcan M. Short communication: influence of restorative material and cement on the stress distribution of posterior resin-bonded fixed dental prostheses: 3D finite element analysis. *J Mech Behav Biomed Mater.* 2019;96:279–84.
- Tiossi R, Vasco MA, Lin L, Conrad HJ, Bezzon OL, Ribeiro RF, et al. Validation of finite element models for strain analysis of implant-supported prostheses using digital image correlation. *Dent Mater.* 2013;29(7):788–96.

**Publisher's note**

Springer Nature remains neutral with regard to jurisdictional claims in published maps and institutional affiliations.